

1849. Neutral network-PID control algorithm for semi-active suspensions with magneto-rheological damper

Cheng Lin¹, Wei Liu², Hongbin Ren³

^{1,2,3}School of Mechanical Engineering, Beijing Institute of Technology, Beijing, 100081, China

^{1,2}Collaborative Innovation Center of Electric Vehicles in Beijing, Beijing, 100081, China

²Corresponding author

E-mail: ¹lincheng@bit.edu.cn, ²diannaolw@126.com, ³renhongbin2106@126.com

(Received 1 July 2015; received in revised form 18 August 2015; accepted 28 August 2015)

Abstract. In this paper, a semi-active suspension control system based on Magneto-Rheological (MR) damper is designed for a commercial vehicle to improve the ride comfort and driving stability. A mathematical model of MR damper based on the Bouc-Wen hysteresis model is built. The mathematical model could precisely describe the characteristics of MR damper compared with the bench test results. The neural network-PID controller is designed for the semi-active suspension systems. According to the numerical results, the proposed controller can constrain vehicle vibrations and roll angle significantly. A detailed multi-body dynamic model of the light vehicle with four semi-active suspensions are established, and an actual vehicle handling and stability tests are carried out to verify the control performances of the proposed controller. It can be concluded that MR semi-active suspension systems can play a key role in coordination between the ride comfort and handling stability for the commercial vehicle.

Keywords: magneto-rheological (MR), semi-active suspension, neutral network-PID.

1. Introduction

A good vehicle suspension system is to isolate the passengers from external road disturbances and internal vibration from engine to improve the ride comfort. The classical suspension is made up of spring, damper elements and a set of mechanical elements which link the suspended vehicle body to wheels. Most current suspension systems are conventional passive types [1], however, vehicle ride comfort and handing stability are conflicting for the traditional passive suspension systems. Good vehicle ride comfort performance can be achieved with soft damping characteristics especially in the range of 4-8 Hz, which is known to be a sensitive frequency range of human body. But the soft damping cannot keep the tire in contact with the road surface and will deteriorate the vehicle safety and stability [2]. Good tune and design of a passive suspension characteristics can to some extend optimize and coordinate the ride comfort quality and stability, but cannot eliminate these compromises thoroughly [3]. With the development of automobile techniques, the controllable suspension attracts more and more attentions in recent years [4-6], such as active and semi-active suspension systems. Advanced active suspensions can offer opportunities for substantial improvements in ride and handling stability as well as overall vehicle posture by exerting independent forces to vehicle body through a computer-controlled force generator, where additional power sources are needed, such as pumps and compressors. This also implies high energy consumption, complexity and additional expense. These drawbacks have limited its development and application in modern automobile industry. Semi-active suspension is a good compromise between active and passive suspension performance, complexity, and expense. The semi-active damper generates force in a passive manner, but the damping forces can be actively controlled. The damping force is modulated in accordance with the operational conditions, which is controlled by certain logic from sensors connected to CPU. It can be adjusted by changing the orifice size or oil viscosity separately or continuously, such as continuously variable dampers, magneto-rheological suspension. In addition, semi-active suspension is more stable and fail-safe; because it still can work under pure passive mode in case of control system

failed. Due to its less energy consumption and better control priorities under extreme driving conditions, it has been considered as a good alternative [7].

A wide range of control techniques have been developed for active and semi-active suspension systems in last two decades. The sky-hook control strategy is proposed by Karnopp, et al. in 1974 [8] and since then many control strategies are proposed based on sky-hook logic. An adaptive semi-active control algorithm combined with the online sprung mass estimation was proposed by Song [9]. Moradi, et al. [10] designed an adaptive PID-sliding-mode fault-tolerant control for full car suspension systems. Some intelligent approaches are also applied in the control because of the nonlinear and uncertainty characteristics of the vehicle, such as genetic algorithms [11]. Although these intelligent approaches have been applied, the mathematical proof for stability is still not to be demonstrated now; and the system stability is especially important for the active suspension systems [12].

In recent years, the controller design for suspension systems with complex nonlinear characteristics and uncertain disturbances becomes a challenging work, and the applications of neural network in the automotive industry have been achieved many remarkable achievements [13-15]. The approximate neural network model can substitute the actual model in many applications especially in control system design. With appropriate off-line training, the neural network controller can achieve a good coordination between ride comfort and handing stability for the semi-active suspensions [16, 17].

The contribution of this paper is to propose a neural network controller for semi-active suspension system with MR dampers. The full-car model of the light vehicle including suspension and steering system, is built in SIMPACK. A mathematical model of MR damper is established and verified combined with the bench test. Compared with the experimental data, the proposed model is precise. Combined with the neural network-PID control algorithm and mathematical model of MR damper, a closed loop control system for semi-active suspension is proposed.

The rest of paper is organized as following: a nonlinear vehicle model and mathematical model of MR damper are presented in Section 2; while in Section 3 the sky-hook reference model and neutral network-PID control algorithm are introduced in details; the efficacy of the proposed controller is validated by simulation presents in Section 4. Vehicle tests are carried out in Section 5; at the end of the paper, the conclusions are given.

2. Nonlinear dynamic modeling

2.1. Full vehicle model

The full scale vehicle suspension dynamic model is illustrated in Fig. 1. The sprung mass consists of the chassis, which are including passenger and internal components. It connects the suspension systems to four wheels (unsprung masses). The vehicle body is free to heave, pitch, and roll. The four wheels are free to bounce vertically relatively to the vehicle body. The damping forces can be adjusted by controlling the current of MR damper according to designed control logic. m_u is the unsprung mass, which is supported by tire which is modeled as linear spring with stiffness coefficient K_t . The displacement of sprung mass and unsprung mass are denoted as z_s and z_u respectively. A road disturbance is integrated by Gaussian white noise, denoted as q .

The differential equations of the vertical, pitch and roll motions are expressed as:

$$m_s \ddot{z}_s + \sum F_{susij} = 0, \quad ij = fl, fr, rl, rr, \quad (1)$$

$$I_y \ddot{\theta} + a(F_{susfl} + F_{susfr}) - b(F_{susrl} + F_{susrr}) = 0, \quad (2)$$

$$I_x \ddot{\phi} + \frac{B}{2} (F_{susfl} + F_{susrl} - F_{susfr} - F_{susrr}) = 0, \quad (3)$$

where, F_{sus} is the suspension force, which consists of the spring force and damping force, can be

described as:

$$F_{susij} = F(\Delta z_{sij}, \Delta \dot{z}_{sij}, u_{ij}), \quad ij = fl, fr, rl, rr, \quad (4)$$

where, u_{ij} is damping force control current; fl, fr, rl, rr denote front-left, front-right, rear-left, rear-right of the vehicle body.

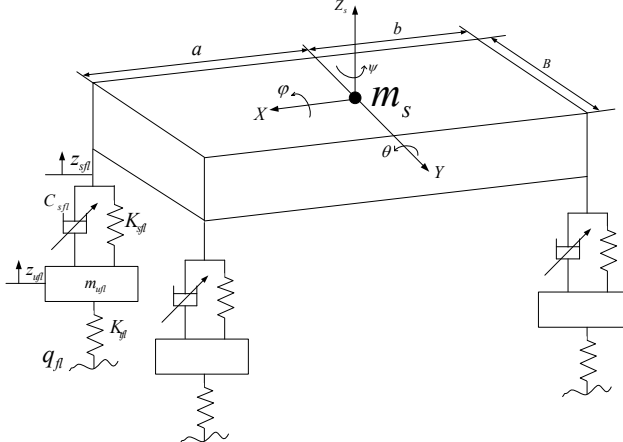


Fig. 1. Full-vehicle semi-active suspension model

The dynamic equations of wheels' vertical motion are as follows:

$$m_{uij}\ddot{z}_{uij} - F_{susij} + k_{tij}(z_{uij} - q_{ij}), \quad ij = fl, fr, rl, rr. \quad (5)$$

Assuming that vehicle body is rigid, and the pitch angle θ and roll angle φ are small, the suspension deflections of four corners are:

$$\begin{aligned} \Delta z_{sfl} &= z_s - a\sin\theta + \frac{B}{2\sin\varphi} - z_{ufl}, \quad \Delta z_{sfr} = z_s - a\sin\theta - \frac{B}{2\sin\varphi} - z_{ufr}, \\ \Delta z_{srl} &= z_s + b\sin\theta + \frac{B}{2\sin\varphi} - z_{url}, \quad \Delta z_{srr} = z_s + b\sin\theta - \frac{B}{2\sin\varphi} - z_{urr}. \end{aligned} \quad (6)$$

2.2. Modeling of MR dampers

A MR damper is a damper filled with magneto-rheological fluid, which can be controlled by a magnetic field. MR fluid is a material that responds to an applied magnetic field with a significant change in its rheological behavior. When the magnetic field is applied, the properties of such a fluid can change from a free-flowing, low viscosity fluid to a near solid, and this change in properties takes place in a few milliseconds and is fully reversible. The damping characteristics of the shock absorber can be continuously controlled by varying the control current of the electromagnet. The MR shock absorber is notably applied in semi-active vehicle suspensions which may adapt to road conditions. The shock absorber is in the form of double tube structure, as shown in Fig. 2. The magnetic intensity of the valve can be adjusted by controlling the current of the coil, and the fluid rheological effect will occur, the damping force could be adjusted continuously. To study the damping characteristics of MR shock absorber, the bench test is carried on under sine excitation, the amplitude is 30 mm, the frequency is 0.3 Hz, and the max velocity is 0.057 m/s. The field current, 0 A, 0.2 A, 0.4 A, 0.6 A, 0.8 A, 1.0 A, 1.5 A, 2 A are applied, as shown in Fig. 3.



Fig. 2. MR damper schematic diagram and physical contrast diagram



Fig. 3. Bench test of MR damper

The nonlinear model of MR damper has been described by many mathematical models, such as Bingham model and nonlinear hysteretic bi-viscous model, et al. [18]. One of the most popular is the Bouc-Wen hysteresis model, originally deduced by Bouc in 1967 and later modified by Wen in 1976 [19]. Later on, Spencer proposed a phenomenological model for MR dampers, a more accurate one based on the Bouc-Wen model [20], shown in Fig. 4. This model predicts the force-displacement behavior of the damper well, and it describes force-velocity behavior that more closely resembles the experimental data. According to the nonlinear force-velocity and force-displacement responses of MR damper, the mathematical model of MR damper can be expressed as:

$$\begin{cases} F_d = c_1 \dot{y} + k_1(x - x_0), \\ \dot{y} = \frac{1}{c_0 + c_1} [\alpha z + c_0 \dot{x} + k_0(x - y)], \\ \dot{z} = -\gamma |\dot{x} - \dot{y}| z |z|^{n-1} - \beta(\dot{x} - \dot{y}) |z|^n + A(\dot{x} - \dot{y}), \end{cases} \quad (7)$$

where, F_d is the damping force of MR damper, and the values of unknown factors ($A, \beta, \gamma, n, c_0, c_1, \alpha, k_0, k_1$) should be determined by test data. The results of parameter identification are obtained by using the optimization algorithm shown in the Table 1.

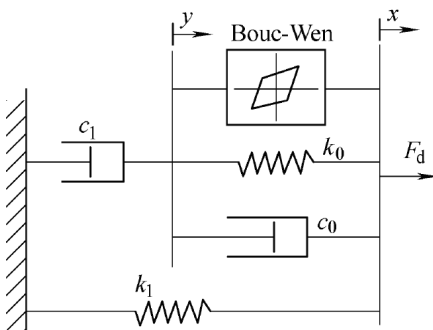


Fig. 4. Bouc-Wen model of MR damper

Table 1. Parameters of Phenomenological model

| Symbols | Values |
|----------|---------------------------|
| A | 31 |
| β | 2.6 mm ² |
| γ | 2.9 mm ⁻² |
| n | 2 |
| c_0 | 29 N·s·mm ⁻¹ |
| c_1 | 1400 N·s·mm ⁻¹ |
| α | 430 mm ² |
| k_0 | -300 Nm |
| k_1 | -298 Nm |

Fig. 5 shows the displacement-force characteristics of the MR shock absorber with the increasing intensity of control current, which implies that the dissipation energy in a vibration cycle would be increasing. Fig. 6 describes the relationship between the damping force and the velocity of the piston-rod of the absorber, when there is no magnetic field applied, the MR fluid would be the Newtonian flow, and the damping force proportionate to the piston-rod velocity; under the same velocity of the piston-rod condition, the damping force would be nonlinear increasing with the current increasing.

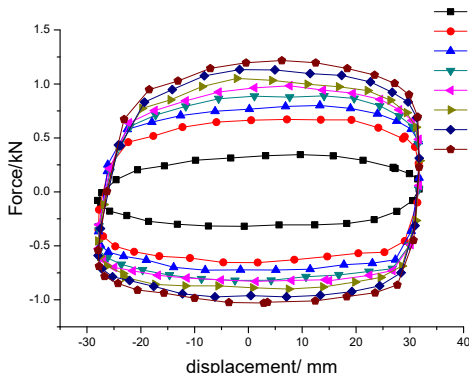


Fig. 5. Displacement-force characteristics of MR damper

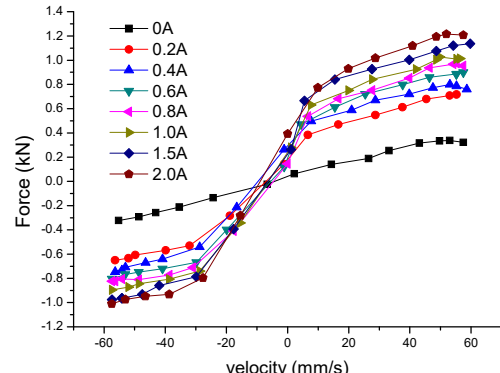


Fig. 6. Velocity-force characteristics of MR damper

Fig. 7 shows the comparison of theoretical and experimental results. It can also be found that the theoretical predictions are in close agreement with the experimental results. It means that the mathematical model can be used to precisely describe the characteristics of the prototype MR damper.

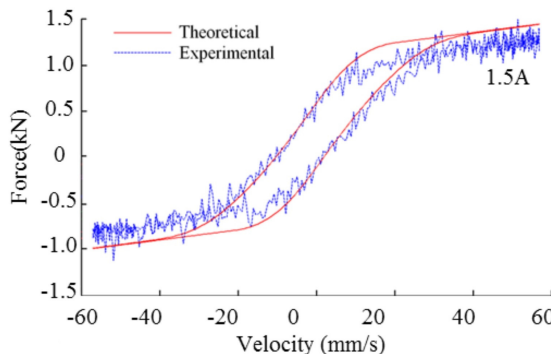


Fig. 7. Comparison of theoretical model and experimental data for MR damper

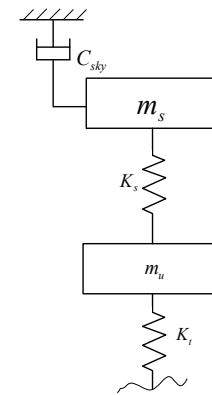


Fig. 8. The configuration of sky-hook reference model

3. Design of semi-active controller

3.1. Sky-hook reference model

The ideal sky-hook is a comfort-oriented control policy. The sky-hook damper control is assumed to be approximately realized by a state feedback control scheme. The sky-hook reference control model is as shown in Fig. 8.

The on-off sky-hook control logic can be expressed as:

$$F_{sky} = \begin{cases} C_{sky}(\dot{z}_s - \dot{z}_u), & \dot{z}_s(\dot{z}_s - \dot{z}_u) > 0, \\ 0, & \dot{z}_s(\dot{z}_s - \dot{z}_u) < 0, \end{cases} \quad (8)$$

where, C_{sky} is the sky-hook damping coefficient.

3.2. Neutral network-PID Control

The aim of semi-active controller is to control the motion of the vehicle body and the vertical

vibration of unsprung masses to adapt different operating conditions. Generally speaking, the ride comfort and handing stability are conflicting for the traditional passive suspension. The main purpose of semi-active controller is to adjust the damping force according to the designed control algorithm determined by the transient suspension states, so as to reduce the vertical vibration of suspension and maintaining proper vehicle body posture. PID control is a more classic control algorithm, composed by the proportional, integral and differential links. When the vehicle roll rate is too large to cause the instability, the incremental PID controller can adjust the damping of suspension to produce a corrected roll moment. However, there are couplings among heave, roll and pitch motion of vehicle, and it is very difficult to improve the ride comfort and handing stability of automobile simultaneously. Therefore, the neural network methodology is adopted here to identify the different driving conditions and adjust the proportional, integral and differential coefficients (K_p , K_i and K_d) of PID controllers. After being trained by using a large amount of sample data, neural network algorithm can predict the state of the vehicle, and make timely and effective control strategy adjust to cope with the road excitation and the state of vehicle changes. Finally, a hybrid damping force control scheme based on PID and neural network control algorithm is proposed, shown in Fig. 9.

According to Eqs. (1)-(7), the system function can be rewritten as:

$$\begin{cases} \dot{\mathbf{x}} = f(\mathbf{x}, \mathbf{u}) + \mathbf{G}\mathbf{q} \\ \mathbf{y} = h(\mathbf{x}), \end{cases} \quad (9)$$

where, $\mathbf{u} = [u_{fl} \ u_{fr} \ u_{rl} \ u_{rr}]^T$ are the damping control forces from control algorithm; \mathbf{q} is the road disturbance input.

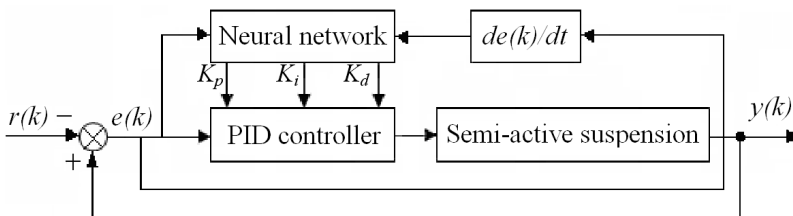


Fig. 9. PID neural network control algorithm block diagram

The input of this control algorithm, shown in Fig. 9, is the tracking errors of ideal value from reference model and actual value, and the output of this control algorithm is the added value of the controlled object. The incremental PID control methodology is adopted in this paper, which provides the damping forces for semi-active suspensions. The PID control algorithm can be expressed as:

$$u(k) = k_p e(k) + k_i \sum_{j=0}^k e(j) + k_d [e(k) - e(k-1)] = u_1(k) + u_2(k) + u_3(k), \quad (10)$$

where, $e(k)$ is the deviation of the actual and reference value; $u(k)$ is the output of PID controller.

Artificial neural network is developed with the biological neural network, and the basic unit of biological neural network is biological neuron, while the artificial neuron is the basic unit of artificial neural networks. Neural network controllers have been expressed in many forms, a frequent representation is a multilayer feed-forward network. In neural network representation, it can be easy to visualize and analyze the signal flow through the incremental PID controllers. A simple neural network control system prototype is shown in Fig. 10. There are two inputs (roll angle and vertical acceleration of vehicle), two input membership functions, and six outputs (proportional, integral and differential coefficients of PID controllers).

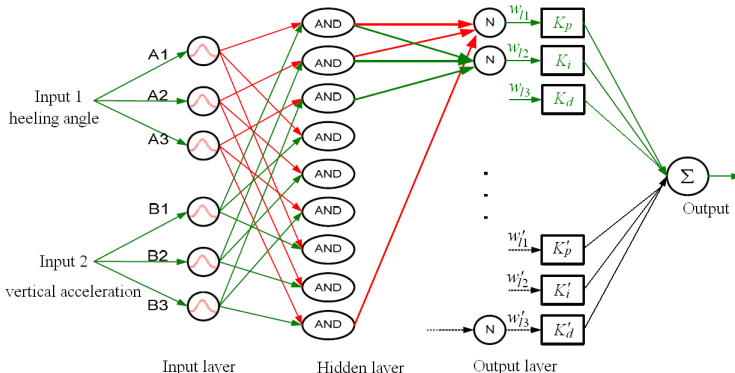


Fig. 10. Neural network control system prototype

Every node in the input layer, which is a membership function, is an adaptive node. There are six input nodes in this layer. $A_1 = e(\varphi)$ is the deviation of the ideal and the actual heeling angle; $A_2 = de(\varphi)/dt$ reflects the rate of change of the deviation; $A_3 = 1$ means the biasing logic. $B_1 = e(a)$ is the deviation of the ideal and the actual acceleration of unsprung mass; $A_2 = de(a)/dt$ reflects the rate of change of the deviation; $A_3 = 1$ means the biasing logic. The output of this node is a matching degree of an input to the corresponding membership functions in the PID set:

$$o_{1,j} = B_i x(j), \quad j = 4, 5, 6, \quad (11)$$

where, $o_{1,j}$ is the membership grade of a PID set.

On the hidden layer, each node represents an “AND” operator, and is a fixed node whose output is the product of the entire incoming signals. The inputs and outputs of hidden layer can be expressed as:

$$net_i^p = \sum_{j=1}^3 w_{ij} o_j^p - \theta_i, \quad (12)$$

$$o_i^p = g(net_i^p), \quad i, j = 1, 2, \dots, 9, \quad (13)$$

where, θ_i is the valve value of the hidden layer. w_{ij} is the connected weights between the input layer and the hidden layer. $g()$ is Sigmoid type active function, that can be expressed as:

$$g(x) = \frac{1}{1 + \exp\left[-\frac{x + \theta_1}{\theta_0}\right]}, \quad (14)$$

where, θ_1 is the parameter represents the biasing value. θ_0 is used for regulating the shape of the Sigmoid function.

The input of the output layer is:

$$net_l^p = \sum_{i=1}^4 w_{li} o_i^p - \theta_l, \quad i, j = 1, 2, \dots, 6, \quad (15)$$

where, w_{li} is the connection weights of the hidden layer neuron i and the output layer neuron l ; θ_l is the valve value of the output layer neuron.

The outputs of the output layer correspond to the three parameters of PID controller, K_p , K_i

and K_d . The basic principle of learning algorithm is the gradient steepest descent method, that is, adjust the weights of the network to make the error of network to a minimum. Select the performance index function as follows:

$$J_p = \sum_{k=1}^3 e^2(k). \quad (16)$$

According to gradient method, the correction formula of the connection weights of output layer neurons is:

$$\Delta w_{li} = -\eta \frac{\partial J_p}{\partial w_{li}} = -\eta \frac{\partial J_p}{\partial net_l^p} \frac{\partial net_l^p}{\partial w_{li}}, \quad (17)$$

where, η is the learning rate, $\eta > 0$. The connection weights of output layer can be expressed as:

$$\Delta w_{li} = -\eta \frac{\partial J_p}{\partial net_l^p} \frac{\partial}{\partial w_{li}} \left(\sum_{i=1}^4 w_{li} o_i^p - \theta_l \right) = -\eta \frac{\partial J_p}{\partial net_l^p} o_i^p. \quad (18)$$

According to gradient method, the correction formula of the connection weights of hidden layer neurons is:

$$\Delta w_{ij} = -\eta \frac{\partial J_p}{\partial w_{ij}} = -\eta \frac{\partial J_p}{\partial net_i^p} \frac{\partial net_i^p}{\partial w_{ij}}. \quad (19)$$

The connection weights of hidden layer can be expressed as:

$$\Delta w_{ij} = -\eta \frac{\partial J_p}{\partial net_i^p} \frac{\partial}{\partial w_{ij}} \left(\sum_{i=1}^3 w_{ij} o_j^p - \theta_i \right) = -\eta \frac{\partial J_p}{\partial net_i^p} o_j^p. \quad (20)$$

The formula of the connection weights of output and hidden layer neurons l and i under the training of sample p can be expressed as:

$$w_{li}(k+1) = w_{li}(k) + \Delta w_{li}, \quad (21)$$

$$w_{ij}(k+1) = w_{ij}(k) + \Delta w_{ij}. \quad (22)$$

4. Simulation and discussion

The virtual prototyping models of front and rear suspension are established in SIMPACK software. MR damper is an important part of this model, and the damping force can be controlled by semi-active suspension. The Magic Formula tire force model is used in SIMPACK. The outs of the tire are obtained from the look-up-table provided by tire tests. The light vehicle model including driver model, suspension and steering systems is shown in Fig. 11.

To simulate the ride comfort and handing stability of the light bus, a neural network controller and virtual prototyping model of automobile are established respectively in MATLAB and SIMPACK software. By defining the data exchange interface between the integrated controller and the virtual prototyping model, the control of semi-active suspensions is achieved in simulation environment. The SIMPACK software, contains various kinds of random roads, has been used in simulation tests. And the interface standard provided by SIMPACK/SIMAT makes the co-simulation with MATLAB software. The four MR dampers with adjustable damping

coefficient are controlled by the neural network PID control algorithm. The communication interface between the software makes the connection between physical models of the dampers and controller possible. In the cooperating applications, there are three signal transmission paths. In the first path, the physical model of full-car passes the values required by neural network controller through the SIMAT module of SIMPACK. Then, the neural network controller analyzes the input signals and makes an output signal to control the intensity of currents. The magnetic intensity of MR damper model is controlled by the input currents, in the end, the forces of dampers reactions outputted by MR damper model is entered into the semi-active suspension of the full-vehicle model, as shown in Fig. 12.

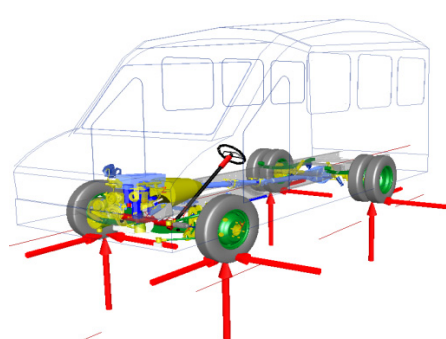


Fig. 11. Dynamic multi-body model of vehicle

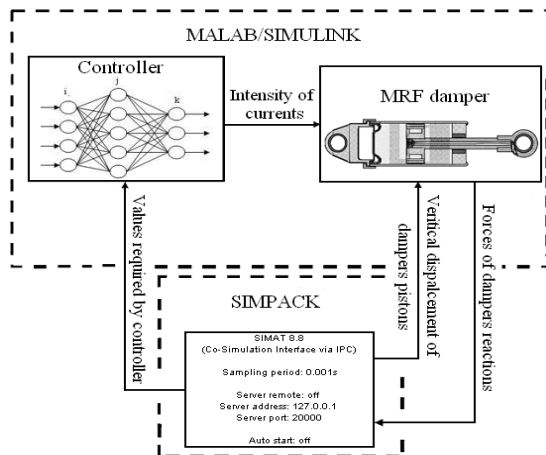


Fig. 12. Block diagram of MATLAB and SIMPACK co-simulation

In order to verify the control performances of neural network-PID control strategy, the passive and semi-active suspension vehicle are compared. In ride comfort simulation conditions, the speed is kept constant as 80 km/h driving on grade B road. In this situation, the vertical, pitch and roll acceleration of vehicle body are tested to verify the control performance of semi-active suspensions.

The power spectral density (PSD) comparison of the vertical, pitch and roll acceleration curves are plotted in Fig. 13. We can find that the PSD amplitude of semi-active suspensions is much smaller than passive suspension. It clearly indicates that the semi-active suspensions controlled by neural network controller could be better coordinate the ride comfort and handling stability compared with the passive suspension.

In order to evaluate the handling performance of the control algorithm, a sine wave test is carried out. The vehicle speed is kept constant as 50 km/h, and the roll angle and yaw angular velocity of vehicle body are tested to verify the effect of semi-active suspensions (see Fig. 14, red line – time domain curve of passive suspension, black line - time domain curve of semi-active suspension). As seen from the simulation results, with the application of semi-active suspensions, the magnitude of heeling angle and yaw angular velocity of vehicle body has been effectively constrained.

5. Test results analysis

The prototype vehicle is equipped with four MR dampers. The control systems include four acceleration sensors, A/D and D/A boards, dSPACE Auto-Box control system with the control software, four MR dampers and four electronic current drivers which provide control current and a data acquisition instrument. The acceleration sensors are used to measure the vertical accelerations of the front and rear sprung masses. The location of acceleration sensors placements are shown in Fig. 15.

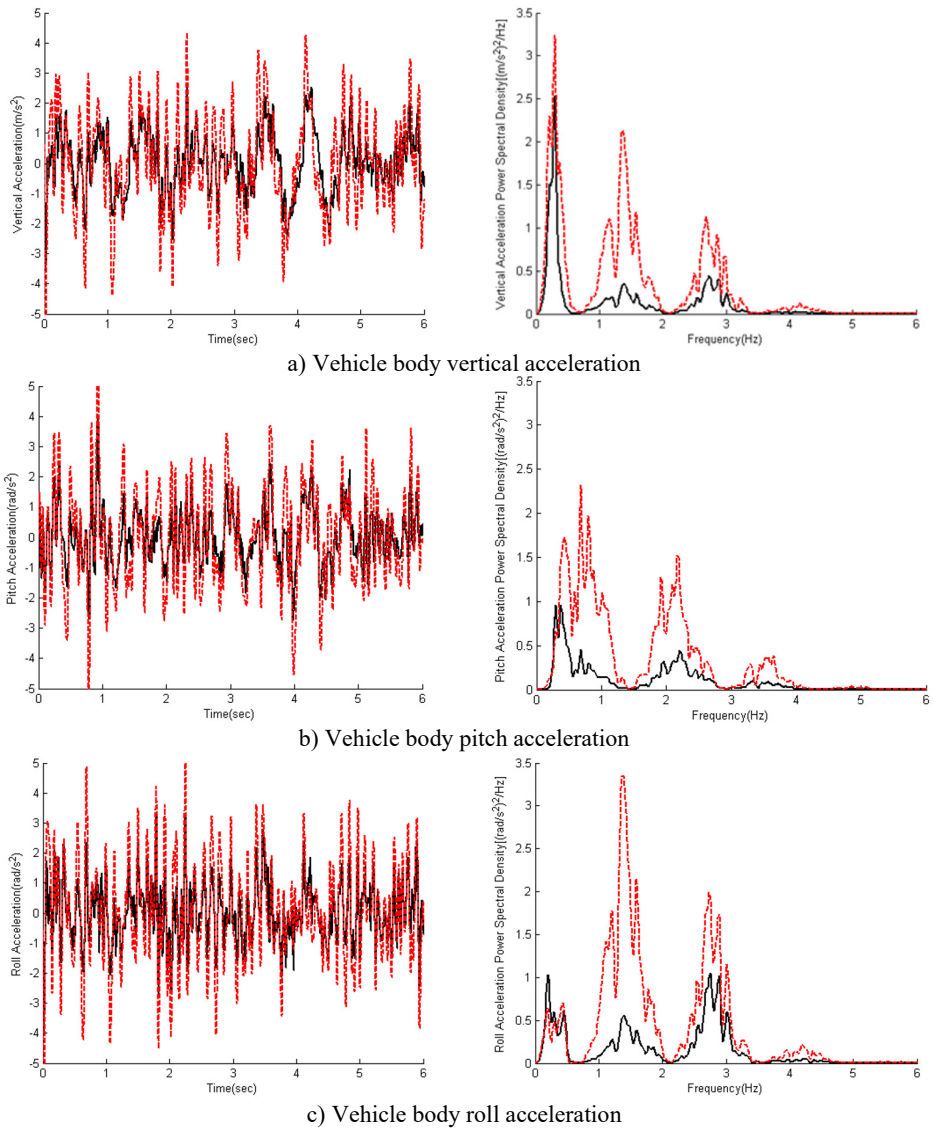


Fig. 13. Time history and PSD analysis results of vehicle body vibration (dotted line – passive suspension PSD results, continuous line – semi-active suspension PSD results)

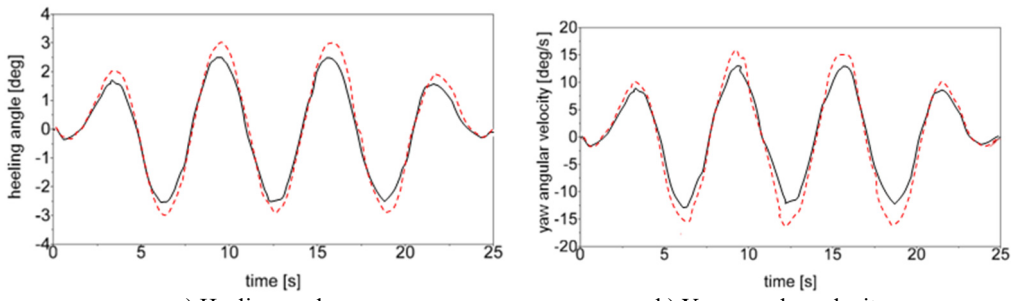


Fig. 14. Time history of snaking motion simulation (dotted line – passive; continuous line – semi-active)

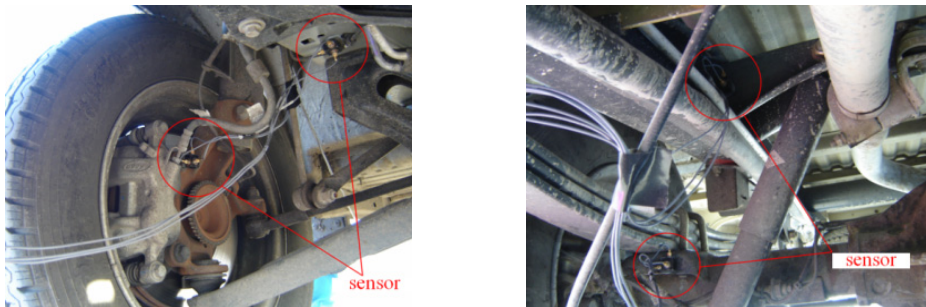


Fig. 15. Location of acceleration sensors

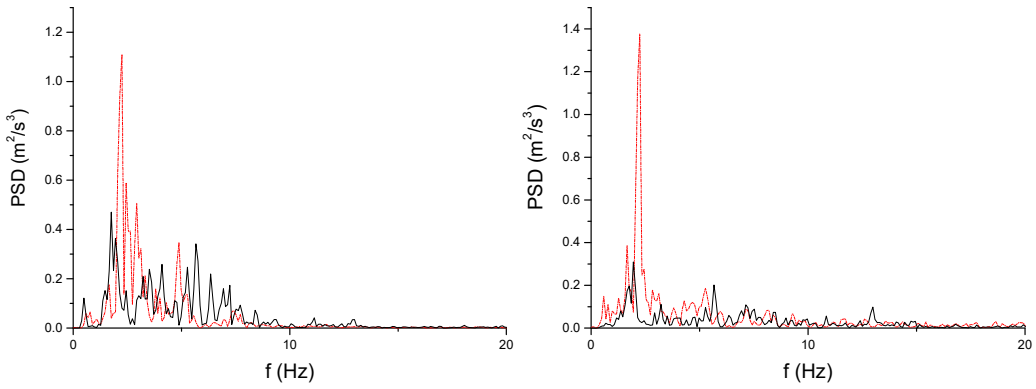


Fig. 16. Vertical acceleration test results ((dotted line – passive; continuous line – semi-active))



Fig. 17. Handing stability test

The vehicle speed is kept constant as 80 km/h driving on a random highway road, and the vertical acceleration comparison of driver seat and vehicle body center are shown in Fig. 16.

The handing stability testing of the light vehicle with semi-active suspensions is shown in Fig. 17. In addition to the testing instruments used in the ride comfort experiment, an equipment called Gyro instrument was used to test the roll and yaw angular velocity of vehicle body. In the handing stability test, six stakes were layout on the test site (30 m spacing), and the test vehicle passed through all stake at the constant speed of /h.

The heeling angle and yaw angular velocity of vehicle body are shown in Fig. 18 (dotted line – passive suspension simulation results, continuous line – semi-active suspension simulation results)). As seen from the Fig. 18, the semi-active controller applied on MR dampers effectively reduces the roll and yaw angle of vehicle body, and the effect of semi-active suspension has been reflected in the handing stability test.

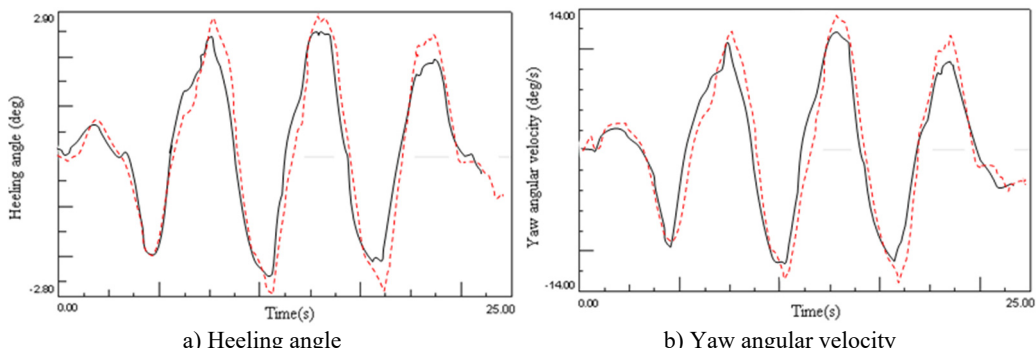


Fig. 18. Experimental results of handing stability ((dotted line – passive; continuous line – semi-active)

6. Conclusion

A full-vehicle semi-active suspension control system equipped with four MR dampers has been developed in the paper. The Neural network-PID control algorithm is proposed for the semi-active suspension systems. The numerical simulation and experiments test results demonstrated that semi-active suspension can effectively attenuate the vertical vibration and the pitch, roll motion of vehicle body. It can be concluded from the obtained results that the semi-active suspension with MR damper can improve the ride comfort and handling performance of automobile simultaneously.

Acknowledgements

The project is supported by the National Sci-Tech Support Plan (Grant No. 2014BAG02B02).

References

- [1] **Tseng H. Eric, Davor Hrovat** State of the art survey: active and semi-active suspension control, Vehicle System Dynamics, Vol. 53, Issue 7, 2015, p. 1034-1062.
- [2] **Hong K. S., Sohn H. C., Hedrick J. K.** Modified skyhook control of semi-active suspensions: a new model, gain scheduling, and hardware-in-the-loop tuning. Journal of Dynamic Systems, Measurement, and Control, Vol. 124, Issue 1, 2012, p. 158-167.
- [3] **Ahmadian M. E. H. D. I., David E. Simon** An analytical and experimental evaluation of magneto rheological suspensions for heavy trucks. Vehicle System Dynamics, Vol. 37, 2003, p. 38-49.
- [4] **Lajqi Shpetim, Stanislav Pehan** Designs and optimizations of active and semi-active non-linear suspension systems for a terrain vehicle. Strojnicki vestnik – Journal of Mechanical Engineering, Vol. 58, Issue 12, 2012, p. 732-743.
- [5] **Tchamna Rodrigue, Edward Youn, Iljoong Youn** Combined control effects of brake and active suspension control on the global safety of a full-car nonlinear model. Vehicle System Dynamics, Vol. 52, Issue 1, 2014, p. 69-91.
- [6] **Assadsangabi B., Eghezad M., Daneshmand F., et al.** Hybrid sliding mode control of semi-active suspension systems. Smart Materials and Structures, Vol. 18, Issue 12, 2009, p. 1-10.
- [7] **Kashem Saad Bin Abul, Mehran Ekteabi, Romesh Nagarajah** Comparison between different sets of suspension parameters and introduction of new modified skyhook control strategy incorporating varying road condition. Vehicle System Dynamics, Vol. 50, Issue 7, 2012, p. 1173-1190.
- [8] **Karnopp D., Crosby M. J., Harwood R. A.** Vibration control using semi-active force generators. Journal of Manufacturing Science and Engineering, Vol. 96, Issue 2, 1974, p. 619-626.
- [9] **Song X., Ahmadian M., Southward S., et al.** An adaptive semiactive control algorithm for magnetorheological suspension systems. Journal of Vibration and Acoustics, Vol. 127, Issue 5, 2005, p. 493-502.
- [10] **Moradi Morteza, Afef Fekih** Adaptive PID-sliding mode fault tolerant control approach for vehicle suspension systems subject to actuator faults. IEEE Transactions on Vehicular Technology, Vol. 63, Issue 3, 2014, p. 1041-1054.

- [11] **Sun L., Cai X., Yang J.** Genetic algorithm-based optimum vehicle suspension design using minimum dynamic pavement load as a design criterion. *Journal of Sound and Vibration*, Vol. 301, Issue 1, 2007, p. 18-27.
- [12] **Chiang H., Lee L.** Optimized virtual model reference control for ride and handling performance-oriented semi-active suspension systems. *IEEE Transactions on Vehicular Technology*, Vol. 64, Issue 5, 2015, p. 1679-1690.
- [13] **Cong S., Liang Y.** PID-like neural network nonlinear adaptive control for uncertain multivariable motion control systems. *IEEE Transactions on Industrial Electronics*, Vol. 56, Issue 10, 2009, p. 3872-3879.
- [14] **Hahm D., Koh H.-M., Ok S.-Y., Park W., Chung C., Park K.-S.** Cost-effectiveness evaluation of MR damper system for cable-stayed bridges under earthquake excitation. *Proceedings of the 3rd International Conference on Bridge Maintenance, Safety and Management – Bridge Maintenance, Safety, Management, Life-Cycle Performance and Cost*, 2006, p. 301-302.
- [15] **Guo A. X., Cui L. L., Li H.** Structural control of seismically induced pounding of elevated bridges by using magnetorheological dampers. *Proceedings of the 3rd International Conference on Bridge Maintenance, Safety and Management – Bridge Maintenance, Safety, Management, Life-Cycle Performance and Cost*, 2006, p. 685-686.
- [16] **Ramli R., Pownall M., Levesley M., Crolla D. A.** Dynamic analysis of semi-active suspension systems using a co-simulation approach. *Multi-Body Dynamics: Monitoring and Simulation Techniques-III*, Vol. 32, Issue 4, 2004, p. 391-399.
- [17] **Lee S. H., Hwang Y. S.** A study on a scenario using the PID method. *Progress in Nuclear Energy*, Vol. 51, Issue 2, 2009, p. 253-257.
- [18] **Hong S. R., Wereley N. M., Choi Y. T., Choi S. B.** Analytical and experimental validation of a nondimensional Bingham model for mixed-mode magnetorheological dampers. *Journal of Sound and Vibration*, Vol. 312, Issue 3, 2008, p. 399-417.
- [19] **Wen Y. K.** Method for random vibration of hysteretic systems. *Journal Engineering Mechanics*, Vol. 102, Issue 2, 1976, p. 249-263.
- [20] **Spencer B. F., Jr. Dyke S. J., Sain M. K., Carlson J. D.** Phenomenological model of magnetorheological dampers. *Journal of Engineering Mechanics*, Vol. 123, Issue 2, 1996, p. 230-238.



Cheng Lin is Director and Professor at Beijing Institute of Technology. His main research directions include: electric vehicle technology, electric vehicle integration theory, optimization and lightweight body structure. His current positions include: China Society of Automotive Engineering Member, SAE member, China Energy Society executive director, Beijing Electric Vehicle Society of Automotive Engineering group leader, US international journal's International Journal of Powertrains (IJPT) editorial.



Wei Liu received Doctor's degree in Vehicle Engineering from Jilin University, Changchun, China, in 2012. Now he is a post-doctor student at Beijing Institute of Technology, Beijing, China. His current research interests include vehicle dynamics and control.



Hongbin Ren received B.S. degree in Mechanical Engineering from Taiyuan University of Technology, Taiyuan, China, in 2010. Now he is a Ph.D. student at Beijing Institute of Technology, Beijing, China. His current research interests include vehicle dynamics and suspension control.